10.1071/WF24161
International Journal of Wildland Fire

Supplementary Material

Assessing wildland fire suppression effectiveness with infrared imaging on experimental fires

Melanie Wheatley[A,*,§], *Joshua M. Johnston*[B], *B. Mike Wotton*[A,B], *Douglas G. Woolford*[C] and *David L. Martell*[A]

[A]Institute of Forestry and Conservation, John H. Daniels Faculty of Architecture, Landscape and Design, University of Toronto, Toronto, ON M5S 3B3, Canada

[B]Great Lakes Forestry Centre, Canadian Forest Service, Natural Resources Canada, Sault Ste Marie, ON P6A 2E5, Canada

[C]Department of Statistical and Actuarial Sciences, University of Western Ontario, London, ON N6A 5B7, Canada

*Correspondence to: Email: melanie.wheatley@ontario.ca

Appendix A

Overview of infrared imaging data processing procedures used to produce the following fire behaviour attributes: rate of spread (m/min), fire radiative power (FRP in kW), FRP density (FRPD) in kW/m^2, fire radiative energy density (FRED) in kJ/m^2, and fireline intensity (kW/m).

Rate of spread

Forward rate of spread was estimated by calculating the interval between arrival times at adjacent pixels. The fire arrival time at individual pixels was estimated based on a temperature threshold of 773 K (e.g., Johnston et al., 2018), specifically when each pixel reached a radiant temperature of 773 K as estimated by the sensors for two consecutive time frames, this was determined to be the time when the fire arrived at the pixel. This method locates all pixels along the leading perimeter of the flame front at the identified threshold and then uses a time series of flame front perimeters to determine the direction of spread at each pixel. The distances travelled between the successive perimeters in the time series of images are used to calculate rate of spread at each pixel along the flame front. In practice, this was accomplished through the following steps: generating the arrival time map for all pixels; interpolating arrival times for unassigned pixels (i.e., pixels that did not reach a temperature threshold of 773K); using the fire perimeter time series, which essentially defines an 'arrival time surface' to calculate the local gradient of the 'arrival time surface' at each pixel; and then converting the slope of this arrival time surface into ROS (m/min). This method of calculating fire arrival times and rates of spread was found to provide rate of spread estimates that are comparable to those obtained using traditional ground sampling methods based on the use of thermocouples in Johnston et al., (2018). This estimated rate of spread for each pixel is representative of the spread rate of the fire at the time the fire arrived in the pixel (Figure 2b in main text).

Fire radiative power

Similar to Johnston et al., (2018), Fire Radiative Power (FRP; W) was computed using the MWIR radiance method as described by Wooster et al., (2003; 2005). The brightness temperature (K) value in each pixel was converted to spectral radiance units ($W/m^2/sr/\mu m$) using the MWIR camera's spectral response function and the Planck function. The FRP was then reported in terms of Watts per pixel for each time interval in the data (i.e., every half second), and is an estimate of the radiative power emitted by the pixel.

Fire radiative energy density

Fire radiative energy density (FRED; kJ/m^2) represents the spatially explicit total radiative energy released from the combustion of the fuels in each pixel. FRED was computed by temporally integrating the FRP (kW) at each pixel over the full duration of burning and scaling to account for pixel area (m^2). Given that FRED is an estimate of the radiative energy release captured by the IR camera from the combustion of fuels in each pixel, it can be scaled to provide an estimate of the total energy release by using a pre-defined radiative fraction estimated to be ~ 0.15 based on Johnston et al., (2017).

Fireline intensity

Fireline intensity was calculated using the methods described in Johnston et al., (2017), a method that has been compared to traditional ground sampling methods at this site specifically. The fireline intensity is the product of the rate of spread and FRED in each pixel, while accounting for a radiative fraction. The fireline intensity is expressed in kW/m for each spatial pixel and because Byram's fireline intensity is a measure of the energy released per second from the entire flame depth, the energy released from the pixel over the duration of the passage of the fire through the pixel must be integrated.

Appendix B

Table B1. Pre and post-suppression rate of spread (ROS) in m/min and fireline intensity in kW/m for each observation and suppression tactic. Observation reflects the two 'rows' of the burn pad that were analyzed independently (i.e., Row 2 and Row 3 on Figure 3 in the main text).

Burn number	Obser-vation	Suppression tactic	Pre-suppression ROS (m/min)	Post-suppression ROS (m/min)	Δ ROS (m/min)	Pre-suppression fireline intensity (kW/m)	Post-suppression fireline intensity (kW/m)	Δ fireline intensity (kW/m)
B1	1	Direct	1.44	0.04	1.40	82	3	79
B1	2	Direct	0.68	0.27	0.41	64	41	23
B1	1	Indirect	0.39	0.17	0.22	47	25	22
B1	2	Indirect	0.28	0.22	0.06	31	41	-10
B2	1	Direct	0.20	0.11	0.09	20	32	-12
B2	2	Direct	0.27	0.10	0.17	28	11	17
B2	1	Indirect	1.18	0.54	0.64	173	97	76
B2	2	Indirect	0.88	1.22	-0.34	101	95	6
B3	1	Direct	0.50	0.24	0.26	64	38	26
B3	2	Direct	1.18	0.06	1.12	127	1	126
B3	1	Indirect	0.41	0.31	0.10	91	57	34
B3	2	Indirect	0.24	0.36	-0.12	54	61	-7
B4	1	Direct	0.05	0.06	-0.01	25	16	9
B4	2	Direct	0.16	0.07	0.09	38	46	-8
B4	1	Indirect	0.62	0.18	0.44	123	38	85
B4	2	Indirect	0.47	0.25	0.22	207	54	153
B5	1	Direct	0.16	0.30	-0.14	20	61	-41
B5	2	Direct	0.17	0.07	0.10	47	37	10
B5	1	Indirect	0.10	0.14	-0.04	42	45	-3
B5	2	Indirect	0.20	0.16	0.04	47	28	19
B6	1	Direct	0.47	0.11	0.36	66	7	59
B6	2	Direct	0.80	0.43	0.37	146	65	81
B6	1	Indirect	0.14	0.08	0.06	30	14	16
B6	2	Indirect	0.16	0.15	0.01	36	29	7

B7	1	Direct	0.14	0.03	0.11	15	3	12
B7	2	Direct	0.20	0.05	0.15	22	0	22
B7	1	Indirect	0.27	0.09	0.18	33	9	24
B7	2	Indirect	0.15	0.07	0.08	21	10	11
B8	1	Direct	0.68	0.72	-0.04	193	172	21
B8	2	Direct	0.85	0.60	0.25	273	173	100
B8	1	Indirect	0.87	0.32	0.55	266	92	174
B8	2	Indirect	1.18	0.36	0.82	374	129	245
B9	1	Direct	0.78	0.89	-0.11	167	192	-25
B9	2	Direct	0.92	2.73	-1.81	242	465	-223
B9	1	Indirect	0.73	0.69	0.04	100	148	-48
B9	2	Indirect	1.38	0.90	0.48	289	180	109
B10	1	Direct	0.85	0.62	0.23	126	149	-23
B10	2	Direct	0.59	0.33	0.26	163	73	90
B10	1	Indirect	1.29	0.47	0.82	235	101	134
B10	2	Indirect	1.52	0.45	1.07	280	88	192
B11	1	Direct	0.49	0.37	0.12	80	75	5
B11	2	Direct	1.00	0.37	0.63	156	56	100
B11	1	Indirect	0.33	0.54	-0.21	91	110	-19
B11	2	Indirect	1.37	0.50	0.87	318	124	194
B12	1	Direct	1.62	1.16	0.46	61	264	-203
B12	2	Direct	0.84	0.32	0.52	48	102	-54
B12	1	Indirect	0.47	0.07	0.40	56	10	46
B12	2	Indirect	0.47	0.07	0.40	74	4	70
B13	1	Direct	0.53	2.25	-1.72	28	474	-446
B13	2	Direct	0.86	1.75	-0.89	50	545	-495
B13	1	Indirect	2.04	0.77	1.27	361	263	98
B13	2	Indirect	1.80	1.98	-0.18	343	86	257
B14	1	Direct	0.43	0.14	0.29	37	9	28
B14	2	Direct	0.51	0.13	0.38	52	5	47
B14	1	Indirect	0.63	0.35	0.28	128	110	18

B14	2	Indirect	1.06	1.86	-0.8	240	215	25
B15	1	Direct	2.39	0.55	1.84	411	167	244
B15	2	Direct	2.13	0.35	1.78	239	43	196
B15	1	Indirect	0.92	0.40	0.52	243	109	134
B15	2	Indirect	0.82	0.28	0.54	121	77	44
B16	1	Direct	0.19	0.46	-0.27	18	68	-50
B16	2	Direct	2.41	0.35	2.06	18	40	-22
B16	1	Indirect	0.16	0.14	0.02	14	23	-9
B16	2	Indirect	0.25	0.13	0.12	45	30	15
B17	1	Direct	0.96	0.48	0.48	199	71	128
B17	2	Direct	1.13	0.24	0.89	66	16	50
B17	1	Indirect	0.60	1.00	-0.4	110	246	-136
B17	2	Indirect	1.32	0.46	0.86	262	116	146
B18	1	Direct	2.24	1.01	1.23	382	269	113
B18	2	Direct	2.76	0.70	2.06	525	126	399
B18	1	Indirect	0.97	0.58	0.39	119	97	22
B18	2	Indirect	0.37	0.14	0.23	60	30	30
B19	1	Direct	0.79	0.54	0.25	96	116	-20
B19	2	Direct	1.94	0.35	1.59	391	69	322
B19	1	Indirect	1.43	0.26	1.17	320	29	291
B19	2	Indirect	2.34	0.64	1.7	645	46	599
B20	1	Direct	2.13	1.17	0.96	294	154	140
B20	2	Direct	2.26	0.17	2.09	577	48	529
B20	1	Indirect	0.80	0.10	0.7	165	23	142
B20	2	Indirect	0.95	0.10	0.85	170	34	136
B21	1	Direct	1.10	0.14	0.96	249	6	243
B21	2	Direct	1.27	0.29	0.98	199	40	159
B21	1	Indirect	0.86	0.23	0.63	115	39	76
B21	2	Indirect	0.71	0.18	0.53	209	35	174
B22	1	Direct	1.37	0.85	0.52	154	153	1
B22	2	Direct	1.33	0.25	1.08	242	113	129

B22	1	Indirect	2.20	0.63	1.57	495	96	399
B22	2	Indirect	2.04	0.52	1.52	540	107	433

Appendix C

Summary of Objectives 1 and 2, impact of suppression on fire behaviour for fireline intensity, or FI_{diff}.

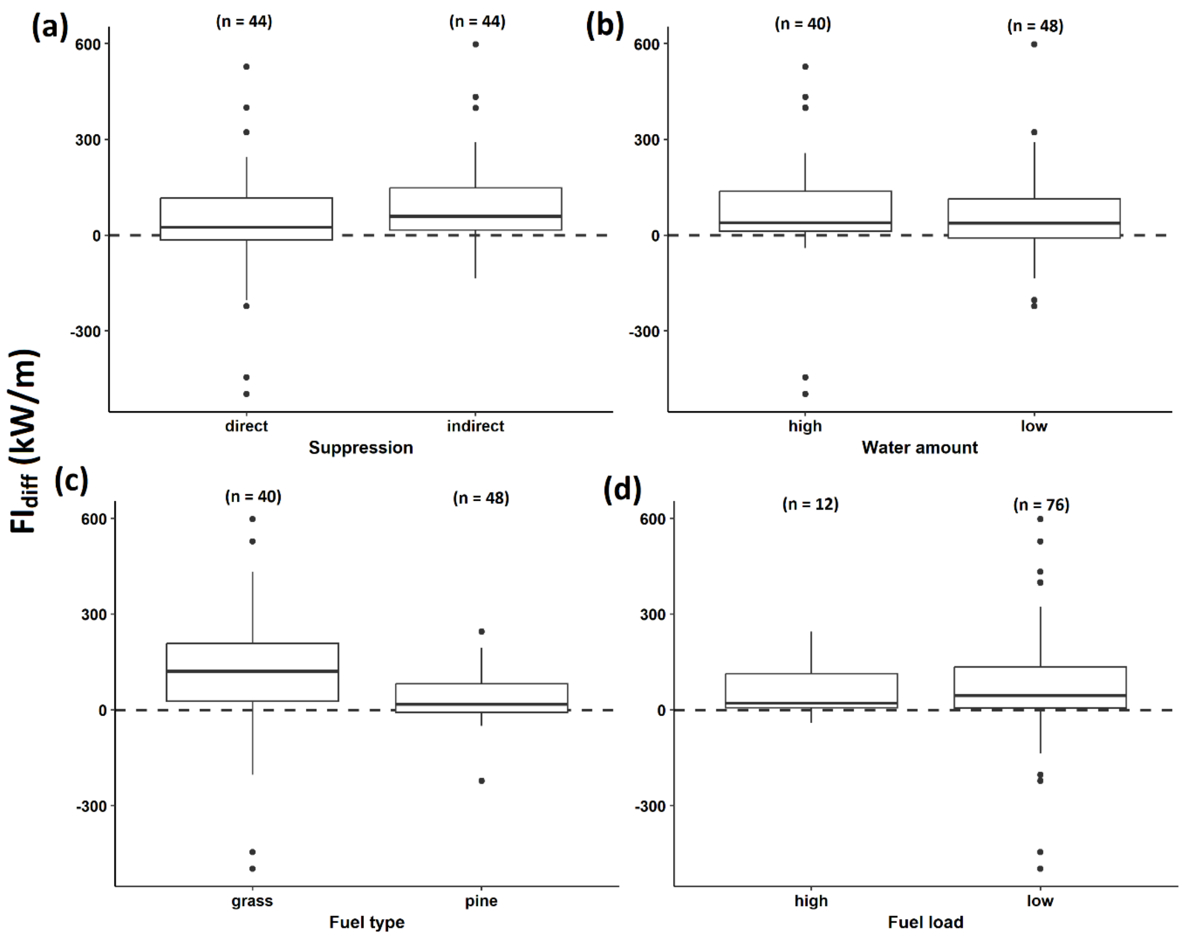

Figure C1. Boxplots of the difference in fireline intensity before and after suppression, FI_{diff} (y-axis, units are kW/m), for each of the four treatment groups examined: (a) suppression, (b) water amount, (c) fuel type, (d) fuel load. The grey dashed line (y = 0 m/min) indicates no change is observed between pre and post suppression treatment. In some cases, the post-suppression fireline intensity was higher than the pre-suppression fireline intensity (as indicated by a negative FI_{diff}).

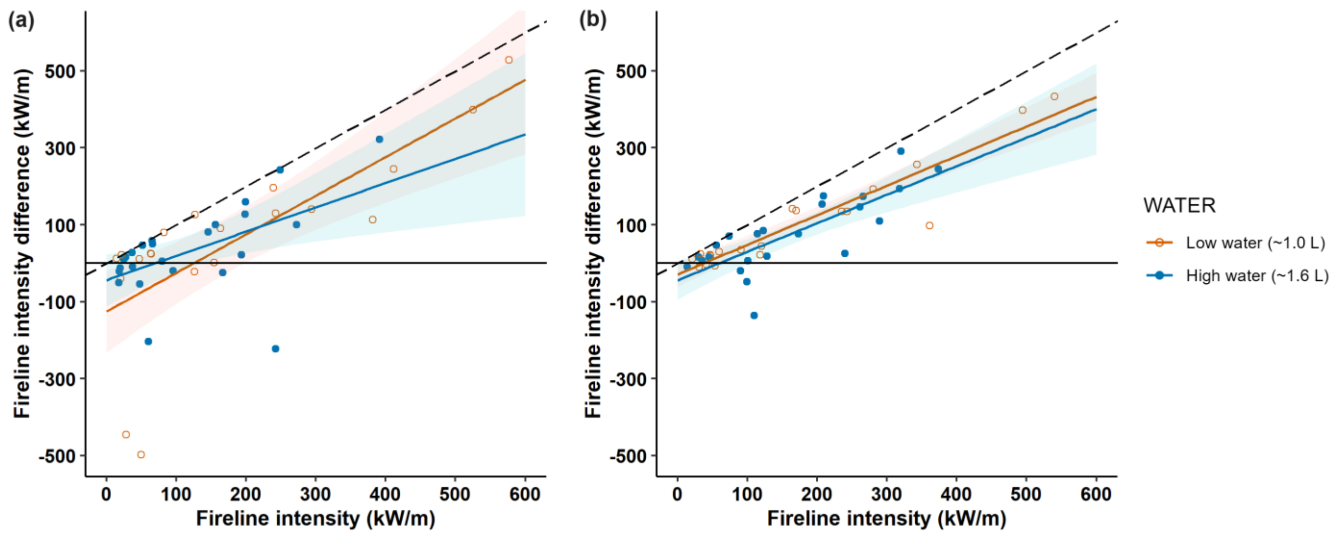

Figure C2. Observations and regression lines of the average fireline intensity before suppression compared to the average FI_{diff} for both **(a)** direct and **(b)** indirect suppression. This figure shows four regressions: one for low and high water for each suppression type. The solid horizontal black line at $y = 0$ represents the theoretical relationship that we would see if suppression did not have any influence on fire behaviour (i.e., the $FI_{diff} = 0$). The dashed $y = x$ line represents the theoretical relationship that we would see if suppression always reduced fireline intensity to 0, indicating that any amount of water applied was fully effective at eliminating intensity.

Table C1. Regression analysis to compare the pre-suppression average fireline intensity and the FI_{diff}. Two generalized linear regression models were fit, one for direct suppression and one for indirect suppression. Interaction terms between pre-suppression fireline intensity (FI) and water amount were included to see if there was evidence that the low and high water amount slopes are different. Table shows the estimates, standard error (s.e) and *p*-values for the coefficients in each model.

		Coefficient (s.e.)		*p*-value
Direct	Intercept	-125.84	(41.90)	0.005
	Pre-suppression FI	1.00	(0.19)	< 0.001
	Water (Low = 1)	81.69	(58.53)	0.17
	Pre-suppression FI × Water	-0.37	(0.31)	0.24
Indirect	Intercept	-29.08	(19.49)	0.14
	Pre-suppression FI	0.77	(0.08)	< 0.001
	Water (Low = 1)	-37.24	(27.30)	0.18
	Pre-suppression FI × Water	0.13	(0.12)	0.27

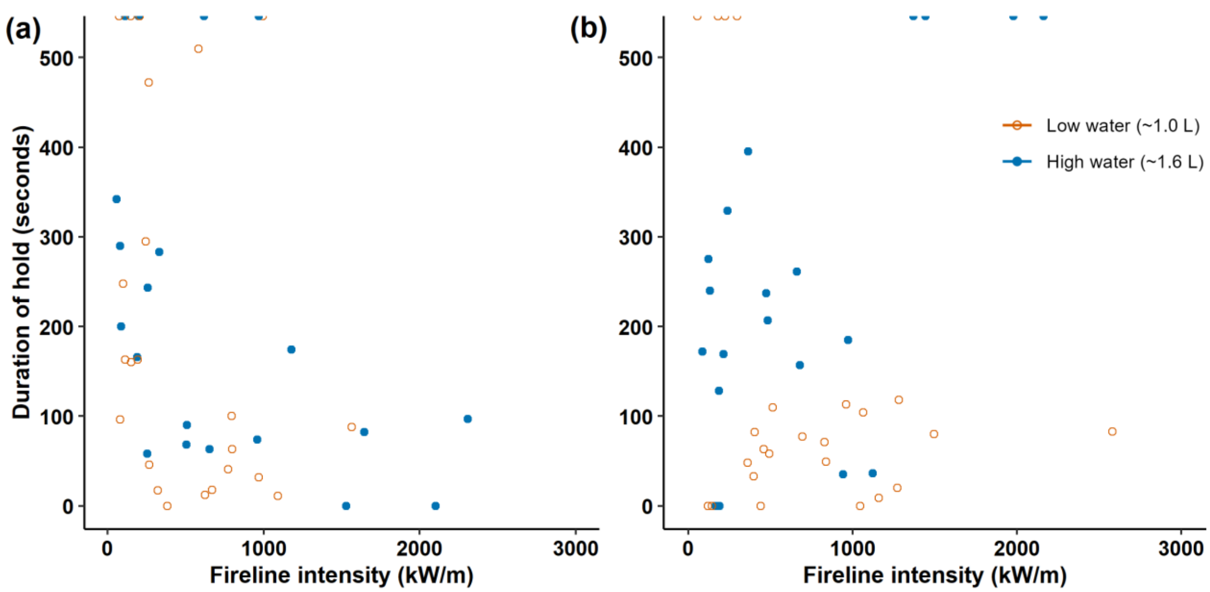

Figure C3. Relationship between the average fire behaviour before suppression and the duration of suppression-inducted fireline hold. (a) the average fireline intensity before suppression and the duration of suppression-induced hold for direct suppression; (b) the average fireline intensity before suppression and the duration of suppression-induced hold for indirect suppression. The points at the top represent observations with a duration of hold set to infinity.